Nitrogen Electric Quadrupole and Proton Magnetic Resonances in Thiourea

David H. Smith and R. M. Cotts

Citation: The Journal of Chemical Physics **41**, 2403 (1964); doi: 10.1063/1.1726278
View online: http://dx.doi.org/10.1063/1.1726278
View Table of Contents: http://scitation.aip.org/content/aip/journal/jcp/41/8?ver=pdfcov
Published by the AIP Publishing

Nitrogen Electric Quadrupole and Proton Magnetic Resonances in Thiourea*

DAVID H. SMITH† AND R. M. COTTS
Labratory of Atomic and Solid State Physics, Cornell University, Ithaca, New York

(Received 7 May 1964)

The nitrogen nuclear electric quadrupole coupling constants for the two nonequivalent thiourea molecules in the low-temperature phase of solid thiourea, $SC(NH_2)_2$, have been determined as a function of temperature between 4° and 169°K. At 77°K, the coupling constants and asymmetry parameters are, for Molecule (1) $e^2q_1Q/h=3121.6$ kc/sec and $\eta_1=0.3954$, and for Molecule (2) $e^2q_2Q/h=3099.6$ kc/sec and $\eta_2=0.3930$. The two highest-frequency transitions in each spectrum exhibit temperature dependences that follow Bayer's theory of electric-field gradient averaging by local oscillators. Zeeman studies place the x principal axis of the electric field gradient out of alignment with the C,N bond, the axis of symmetry in the NH_2 group. Magnetic dipole perturbation coupling between nitrogen and hydrogen nuclei is zero in first order, and the second-order dipole coupling shifts the quadrupole resonance line near values of the Zeeman field, which make the proton Larmor frequency equal to a nitrogen quadrupole transition frequency. The energy-conserving ^{14}N-proton mutual spin flips, which occur at these applied magnetic fields, make several cross-relaxation experiments possible. The temperature dependences of the proton spin–lattice relaxation times is characterized by that of thermally activated molecular reorientation at temperatures above the ferroelectric transition temperature, 169°K. Measured values of the activation energy and pre-exponential frequency factor are 10 kcal/mole and 7.5×10^{13} sec^{-1}. This molecular reorientation inhibits measurement of the quadrupole coupling above 169°K. Nitrogen quadrupole-lattice relaxation times appear to be the same for all level transitions and to follow a T^{-2} temperature dependence between 8° and 165°K.

I. INTRODUCTION

THIOUREA, $SC(NH_2)_2$, is a molecular crystal which exists in solid form below its decomposition temperature of approximately 160°C. The solid exists in five phases as indicated by dielectric susceptibility measurements.[1] The lowest-temperature phase transition at 169°K is of first order as indicated by the anomaly in the specific-heat measurements.[2]

In all of its phases the crystal structure is orthorhombic with four molecules per unit cell and exhibits C_{2v} symmetry in Phase I and D_{2h} symmetry in Phase V.[1,2] An x-ray analysis performed by Goldsmith and White at 120°K[1] (Phase I), indicates that the heavy atoms, S, C, and N, in the molecule form a planar array and that they are arranged as shown in Fig. 1. The x-ray analysis performed at room temperature (Phase V) by Wyckoff and Corey[3] also indicates that the heavy atoms in the molecule are coplanar. The main difference between Phases I and V is the existence of two types of molecular projections onto the bc crystal plane in the former and only one type in the latter. The molecules are positioned in both of the phases so that their dipole moments, about 10 D[2] parallel to the C,S bond, cancel in any given crystalline direction except in Phase I where there is incomplete cancellation of the dipole moment projections along the crystalline b axis (ferroelectric axis). Specifically, at a temperature of 120°K in Phase I, two of the molecular plane normals in the unit cell make angles of 29.5°, while the other two make angles of 19.6° with respect to the b axis.[1] The latter is referred to here as Molecule (1) and the former as Molecule (2). At room temperature the crystal structure is similar except that all molecular normals are at 26.6° relative to the b axis.[3] In all cases, the c axis lies in the plane of the molecules and is perpendicular to their C,S bonds.

Besides showing the coplanarity of the protons with the rest of the molecule, the analysis of the proton magnetic resonance line shapes by Emsley and Smith[4] indicates that the molecular units experience twofold hindered rotation about their C,S bonds in Phase V.

The electric environment around each nitrogen nucleus lacks axial symmetry, and the field gradient could be expected to have a large axial asymmetry parameter η. A large value of η means that the degeneracy of $m=\pm1$ levels of nitrogen ($I=1$) is removed, and the quadrupole energy levels are insensitive to an applied external magnetic field in first-order perturbation theory. It also follows that there is no first-order magnetic dipolar broadening of the nitrogen quadrupole resonance line due to coupling with nearby protons. The effectiveness of the proton–nitrogen dipole–dipole interaction can be changed by application of an external magnetic field. At certain field values, where proton Zeeman splitting equals a nitrogen transition frequency, spin exchange between the two systems can occur. An unexpected, although understood, result is that in this

* This work was supported by the National Science Foundation and the Advanced Research Projects Agency and based partly on the Ph.D. dissertation of David H. Smith, Cornell University, 1963.

† Present address: Bell Telephone Laboratories, Murray Hill, New Jersey.

[1] G. J. Goldsmith and J. G. White, J. Chem. Phys. **31**, 1175 (1959).

[2] H. Futama, J. Phys. Soc. Japan **17**, 434 (1959).

[3] R. W. G. Wyckoff and R. D. Corey, Z. Krist. **81**, 386 (1932).

[4] J. W. Emsley and J. A. S. Smith, Trans. Faraday Soc. **57**, 893, 1233 (1959).

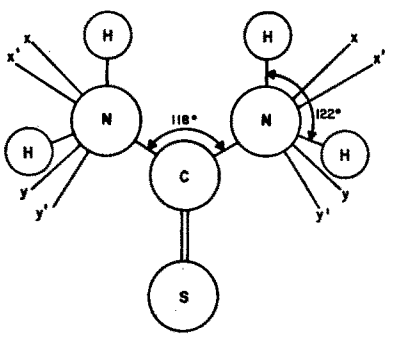

FIG. 1. Arrangement of S, C, and N atoms in thiourea. The anticipated principal axes are labeled (x', y') and the measured principal axes are labeled (x, y).

field region, the proton–nitrogen dipolar interaction *shifts* the nitrogen resonance frequency.

II. EXPERIMENTAL

A Pound–Knight spectrometer[5] modified by the use of capacitance diodes in the tank circuit for sweeping and modulating the frequency of the oscillator was used to detect the nitrogen electric quadrupole resonances in thiourea. If one diode is used for both functions, the frequency-modulation (FM) characteristics change too much as the bias voltage or frequency is swept. Therefore, independent sets of diodes are used for each function in order to avoid large drifts in FM pickup. The capacitance diode bias sweep provided a simple means of insulating the Pound box from microphonic noises generated by the sweep drive motor. The frequency was measured with a Hewlett–Packard 524 D frequency counter.

Nitrogen quadrupole resonances in powdered thiourea are relatively broad (approximately 1 kc/sec) but are only about one third as wide in single-crystal samples. Preliminary work employed powdered thiourea samples to determine the nitrogen quadrupole resonant frequencies from 77° to 169°K and required the use of second harmonic of the modulation-frequency phase-sensitive detection to avoid excessive recorder drift as the frequency was swept. The determinations of resonant frequencies at temperatures below 77°K and principal axis orientations employed single crystals. The narrower lines in the single crystals had higher signal-to-noise ratios, and permitted a smaller modulation so that the first harmonic of the modulation frequency could be detected in the phase-sensitive detector.

Single crystals of thiourea with small occlusions of alcohol were grown from a methanol–thiourea solution by lowering the temperature a few degrees over a period of about eight weeks. The temperature was controlled by a proportional controller[6] having an ac bridge and a thermistor temperature-sensing element.

Single crystals of thiourea are needed for a determination of the electric field gradient principal axis directions and large samples provide good filling factors in low-loss rf coils used at the low nitrogen quadrupole frequencies. To determine the principal axis directions at the nitrogen sites, the orientation dependence of the Zeeman perturbation was studied. The magnetic field was provided by a pair of 12-in.-diam Helmholtz coils mounted on a rotating base. The sample, a large 17.2-g single crystal of thiourea, was oriented in the Pound box probe using the crystal geometry and x-ray structural analysis. The magnetic field was always perpendicular to the c axis and at a known angle relative to the a axis.

A pulsed nuclear magnetic resonance NMR spectrometer ("pulse rig") operated with a pair of sequential 90° pulses[7] was used to measure the spin–lattice relaxation time of the protons in thiourea. The transmitter solenoid, whose axis is perpendicular to that of the receiver coil, has a volume of about 2 cc making it possible to realize an H_1 slightly in excess of 60 G. The temperature of the "pulse-rig" probe was continuously variable from 77° to 400°K and was controlled by the same proportional controller that was used in growing the crystals except that a metallic sensing element was substituted for the thermistor. The "pulse rig" was also used to measure the rate of recovery of the proton polarization, after raising the temperature of the proton system to infinity with 90° pulses, due to cross relaxation with the nitrogen quadrupole system.

III. THEORY

A. Nuclear Electric Quadrupole Interaction

The Hamiltonian for the nuclear electric quadrupole interaction is[8]

$$\mathcal{H}_Q=[e\phi_{zz}Q/4I(2I-1)][3I_z^2-I^2+\tfrac{1}{2}\eta(I_+^2+I_-^2)],$$

where $I_+=I_x+iI_y$, $I_-=I_x-iI_y$, and Q is the electric quadrupole moment of the nucleus. The diagonal crystalline electric field gradient tensor is specified by five parameters, the largest component of the field gradient ϕ_{zz}, the asymmetry parameter η, and the three Euler angles specifying the directions of the principal axis $\eta=(\phi_{xx}-\phi_{yy})/\phi_{zz}$, where $\phi_{zz}\geq\phi_{xx}\geq\phi_{yy}$.

If the eigenfunctions for the three projections of the angular momentum $m_z=1$, 0, and -1 are given by Φ_1, Φ_0, and Φ_{-1}, respectively, then the diagonalized form of the Hamiltonian $\mathcal{H}_Q$ gives the following set of nondegenerate energy levels, E_i, and associated linear combinations of angular-momentum wavefunctions:

$$E_1/\hbar=\omega_Q(1+\eta)/4, \qquad \psi_1=(\Phi_1+\Phi_{-1})(\sqrt{2})^{-1},$$
$$E_2/\hbar=\omega_Q(1-\eta)/4, \qquad \psi_2=(\Phi_1-\Phi_{-1})(\sqrt{2})^{-1},$$
$$E_3/\hbar=-2\omega_Q/4, \qquad \psi_3=\Phi_0,$$

[5] R. V. Pound and W. D. Knight, Rev. Sci. Instr. **21**, 219 (1950).
[6] C. T. Tomizuka and D. Zimmerman, Rev. Sci. Instr. **30**, 40 (1959).
[7] E. Hahn, Phys. Rev. **80**, 580 (1950).
[8] A. Abragam, *The Principals of Nuclear Magnetism* (Oxford Press, London, 1961).

where $\omega_Q=(eQ\phi_{zz})(\hbar^{-1})$. The transitions observed in the experiments performed are those from Levels 1 to 3 and 2 to 3; they are referred to as ν_+ and ν_-, respectively.

B. Zeeman Perturbation of Nuclear Quadrupole Interaction

The new Hamiltonian including quadrupole and Zeeman terms is written in the following way:

$$\mathcal{H}=\mathcal{H}_Q+\mathcal{H}_{Ze},$$

$$\mathcal{H}_{Ze}=-\hbar\gamma_N[H_zI_z+\tfrac{1}{2}H_x(I_++I_-)+\tfrac{1}{2}iH_y(I_--I_+)],$$

where it is assumed that the z principal axis for the crystalline electric field gradient is taken as the axis of quantization in that the quadrupole interaction in the present case is much larger than the Zeeman interaction. The projections of the magnetic field H_0 along the principal axes are H_x, H_y, and H_z; the gyromagnetic ratio of the nitrogen nucleus is given by γ_N. In the representation of the wavefunctions ψ_1, ψ_2, and ψ_3 of the pure quadrupole system, the matrix of the Hamiltonian is

$$(\mathcal{H}/\hbar)=\begin{bmatrix}\omega_Q(1+\eta)/4 & -\gamma_NH_z & -\gamma_NH_x\\ -\gamma_NH_z & \omega_Q(1-\eta)/4 & i\gamma_NH_y\\ -\gamma_NH_x & -i\gamma_NH_y & -2\omega_{Q/4}\end{bmatrix}.$$

Results of a perturbation treatment of the Zeeman interaction on the quadrupole system are given to second order below. Second-order energy shifts (ΔE_1, ΔE_2, and ΔE_3) are

$$\Delta E_1=\frac{4\gamma_N^2\hbar H_0^2}{\omega_Q}\left(\frac{\alpha_x^2}{3+\eta}+\frac{\alpha_z^2}{2\eta}\right),$$

$$\Delta E_2=\frac{4\gamma_N^2\hbar H_0^2}{\omega_Q}\left(-\frac{\alpha_z^2}{2\eta}+\frac{\alpha_y^2}{3-\eta}\right),$$

$$\Delta E_3=\frac{4\gamma_N^2\hbar H_0^2}{\omega_Q}\left(-\frac{\alpha_x^2}{(3+\eta)}-\frac{\alpha_y^2}{(3-\eta)}\right),$$

where α_x, α_y, and α_z are the direction cosines of the magnetic field relative to the principal axis system.

The frequency corresponding to the transitions between 1 and 3 and 2 and 3 labeled ν_+ and ν_- are then as follows:

$$2\pi\nu_+=\tfrac{1}{4}\omega_Q(3+\eta)+\frac{4\gamma_N^2H_0^2}{\omega_Q}\left(\frac{2\alpha_x^2}{3+\eta}+\frac{\alpha_y^2}{3-\eta}+\frac{\alpha_z^2}{2\eta}\right), \quad (1)$$

$$2\pi\nu_-=\tfrac{1}{4}\omega_Q(3-\eta)+\frac{4\gamma_N^2H_0^2}{\omega_Q}\left(\frac{\alpha_x^2}{3+\eta}+\frac{2\alpha_y^2}{3-\eta}-\frac{\alpha_z^2}{2\eta}\right). \quad (2)$$

The frequency shifts of the upper and lower transitions take on the form $\Delta\nu=A(a_1\alpha_x^2+a_2\alpha_y^2+a_3\alpha_z^2)$. The direction cosines α_x, α_y, and α_z, projecting H_0 onto the principal axes, can be expressed in terms of the Euler angles which relate the principal (x, y, z) and crystal

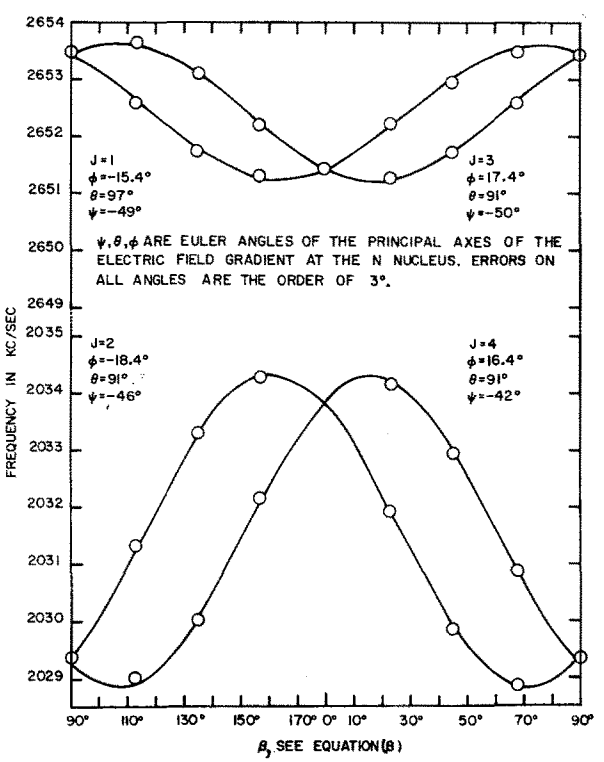

FIG. 2. Zeeman shifts of NQR lines of Molecule (1) versus orientation of H_0. $H_0=159$ G. The angle between H_0 and the a axis in the ab plane is designated β.

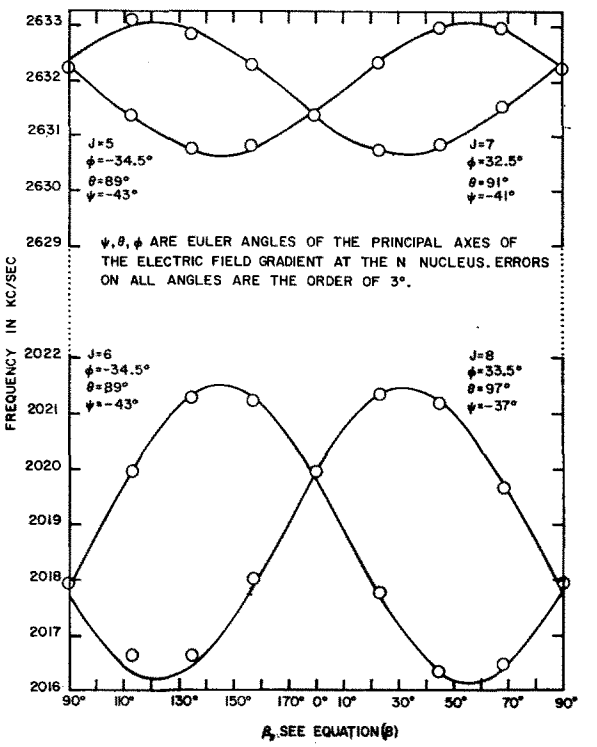

FIG. 3. Zeeman shifts of NQR lines of Molecule (2) versus orientation of H_0. $H_0=159$ G. The angle between H_0 and the a axis in the ab plane is designated β.

TABLE I. Euler angles obtained from Zeeman frequency shift data at 77°K.

Figure	Line (J)	Molecule[a] (deg)	θ (deg)	ϕ (deg)	ψ (deg)	Sum of errors[2] (8 pts.) (kc/sec)^2
2	1	(1) −19.4	97	−15.4	−49	2.99×10^{-2}
2	3	(1) 19.4	91	17.4	−50	8.24×10^{-3}
2	2	(1) −19.4	91	−18.4	−46	1.18×10^{-2}
2	4	(1) 19.4	91	16.4	−42	3.96×10^{-2}
3	5	(2) −29.5	89	−34.5	−43	8.81×10^{-3}
3	7	(2) 29.5	91	32.5	−41	4.1×10^{-2}
3	6	(2) −29.5	89	−34.5	−43	7.17×10^{-2}
3	8	(2) 29.5	97	33.5	−37	0.183

[a] The angles 19.4° and 29.5° are the angles between the normal of the molecular plane and the crystal b axis as determined by Goldsmith and White at 120°K, see Ref. 1.

(a, b, c) axes. Expressions that follow are written for a rotation of H_0 in the ab plane and the angle between H_0 and a axis is β. The Euler angles θ, ϕ, and ψ are labeled in the same way as Goldstein[9] labels them:

$$\alpha_x=\cos\psi\cos(\phi-\beta)-\cos\theta\sin\psi\sin(\phi-\beta),$$

$$\alpha_y=-\sin\psi\cos(\phi-\beta)-\cos\theta\cos\psi\sin(\phi-\beta),$$

$$\alpha_z=\sin\theta\sin(\phi-\beta).$$

With the magnetic field perpendicular to the c axis, each of the observed resonant lines in the thiourea quadrupole spectrum splits into two lines. Each of these lines represents contributions from the nitrogens on one of the two molecules in a particular group. Due to the symmetry of the crystal, splittings will not occur (although a shift can occur) if H_0 is along one of the crystal axes. If H_0 is rotated in another crystal plane each zero-field line will split, but the groupings of physically different nitrogen sites contributing to a particular line will, in general, be different.

For each orientation of H_0 a plot was made of the frequency shift of each nuclear quadrupole resonance (NQR) line vs H_0^2. Each data point on the frequency shift vs orientation of $H_0(\beta)$ is taken from the best straight line drawn through the points of the H_0^2 plot. The rotation patterns of the frequency shifts are given in Figs. 2 and 3.

A Burroughs 220 computer, used to fit the data to Eqs. (1) and (2), employed a least-squares trial-and-error scheme to find the best values of θ, ϕ, and ψ. The angles were changed in steps of 1°, and the standard deviation generally ran around 3°. The results of the fits to the rotation patterns are given in Table I.

The values used for the pure quadrupole parameters are given in Table II for a temperature of 77°K.

IV. DISCUSSION

A. Origins of the Electric Field Gradient

The significance of the measured values of θ, ϕ, and ψ are most readily seen when they are compared to the predictions based on a simplified description of the field gradient and known orientations of the molecules. The field gradient is most strongly influenced by nearby charges so that if it is assumed that the N,H bonds to each N atom are symmetric about the C,N bond, one would conclude that the x (labeled x' in Fig. 1) principal axis would be parallel to the C,N bond, the y (labeled y') principal axis in the NH_2 plane and the z (labeled z') principal axis perpendicular to the NH_2 plane. Then, for the coplanar thiourea molecule,[4] the z principal axis would be parallel to the normal of the molecular plane, and perpendicular to the c axis.

The data in Table III indicate that the xy plane is tipped out of the molecular plane about 2° in the 19.4° molecules and about 4° in the 29.5° molecules. All of the nitrogen sites appear to have field gradients whose z principal axes differ only a few degrees from being perpendicular to the c axis, thus fitting the above simple preconception, primed coordinates, quite well. The greatest deviation from the simple picture appears in a rotation of the axis system x, y, and z about the z axis taking the x axis out of alignment with the C,N bond direction as shown in Fig. 1.

The values of the largest component of the electric field gradient at the nitrogen nucleus ϕ_{zz} and the asym-

TABLE II. Pure quadrupole parameters.

Molecule	ω_Q		A	a_1	a_2	a_3
(1)	3121.6 kc/sec	39.54%	3.06 kc/G^2	$D(0.29452)$[a]	$E(0.28293)$[a]	$F(1.2647)$[a]
(2)	3099.6	39.30	3.09	$D(0.29472)$[a]	$E(0.28359)$[a]	$F(1.2722)$[a]

[a] For high-frequency lines, ν_+, ($J=1, 3, 5, 7$) and, $D=2$, $E=1$, $F=1$. For low-frequency lines ν_-, ($J=2, 4, 6, 8$) and, $D=1$, $E=2$, $F=-1$.

[9] H. Goldstein, *Classical Mechanics* (Addison-Wesley Publishing Company, Reading, Massachusetts, 1950).

TABLE III. Principal axis orientations in the crystal.

Molecule	J	Simple picture prediction ψ (deg)	ϕ (deg)	θ (deg)	Experimental average ψ (deg)	ϕ (deg)	θ (deg)	Deviation $\Delta\psi$ (deg)	$\Delta\phi$ (deg)	$\Delta\theta$ (deg)
(1)	(1, 2)	−59	−19.4	90	−47.5	−16.9	94	−12	−2	4
(1)	(3, 4)	−59	19.4	90	−46	16.9	91	−13	−2	1
(2)	(5, 6)	−59	−29.5	90	−43	−34.5	89	−16	5	−1
(2)	(7, 8)	−59	29.5	90	−39	33	94	−20	4	4

metry parameter η agree qualitatively with estimates based on the three nitrogen bonds in an isolated molecule except that the observed value of η is too large. Charge asymmetry in the molecular plane about the C,N bond could produce the angular shift $\Delta\psi$ of the x axis, and such an asymmetry would also have the effect of increasing the value of η. The same charges which should be effective in rotating the x axis do not contribute materially to ϕ_{zz}. The dipole moment of the molecule does account for some of the charge asymmetry about the C,N bond which leads to a rotation of the x axis from the C,N bond direction. This rotation (12° to 18° depending on the molecule) is larger than would be expected from elementary hybrid atomic bond orbital models and a point charge representation of the dipole moment of the molecule.

It is interesting to note that in the molecule para-bromoaniline, with the NH_2 group attached to a benzene ring, that the observed value of the asymmetry parameter, $\eta=0.23$,[10] is less than in either urea or thiourea where $\eta=0.32$ and 0.40, respectively. The x principal axis in *para*-bromoaniline has been reported[10] to be parallel to the C,N bond, and there is a more symmetric electron environment about the C,N bond in this molecule. If the large value of η in thiourea and the rotational shift of the x axis are correlated, then one might expect that in urea there would also be rotational shift of the x axis.

B. Temperature Dependences of Pure Quadrupole Spectra

The Bayer theory[11,12] of electric field gradient averaging by Einstein local harmonic oscillators is found to be in good agreement with the quadrupole frequency temperature dependences observed. The normalized theoretical curves and data are shown in Figs. 4 and 5.

If the local oscillators are described in terms of angular displacements θ_x, θ_y, and θ_z about the three axes of a stationary coordinate system the stationary system is the average position of the principal axes; therefore, all the off-diagonal elements of the field gradient in the stationary system created by the oscillation described have time-average zero.

The time-averaged NQR frequencies written in terms of the time-average values of the maximum field-gradient component and asymmetry parameter $\langle\phi_{zz}\rangle$ and $\langle\eta\rangle$ are as follows:

$$\nu_+=(e\langle\phi_{zz}\rangle Q/4h)(3+\langle\eta\rangle)=\nu_+'(1-\langle\theta_y^2\rangle-2\langle\theta_x^2\rangle)-\nu_\pm'(\langle\theta_z^2\rangle-\langle\theta_y^2\rangle), \quad (3)$$

$$\nu_-=(e\langle\phi_{zz}\rangle Q/4h)(3-\langle\eta\rangle)=\nu_-'(1-\langle\theta_x^2\rangle-2\langle\theta_y^2\rangle)+\nu_\pm'(\langle\theta_z^2\rangle-\langle\theta_x^2\rangle), \quad (4)$$

where $\nu_\pm'=\nu_+'-\nu_-'$. The primed frequencies ν_+', ν_-', and $\nu_\pm'$ are the NQR frequencies that would be observed if the field-gradient oscillations were absent. The characteristic form of the temperature dependence will in general involve 6 parameters. In order to simplify the fitting of Equations (3) and (4) to the data in Figs. 4

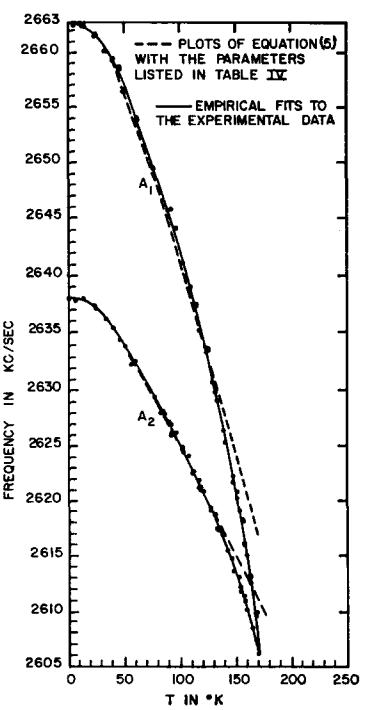

FIG. 4. Temperature dependence of the high-frequency quadrupole resonance of Molecules (1) and (2) in thiourea.

[10] M. Minematsu, J. Phys. Soc. Japan **14**, 1030 (1959).
[11] H. Bayer, Z. Physik **130**, 227 (1951).
[12] T. P. Das and E. L. Hahn, Solid State Phys. Suppl. **1**, 39 ff. (1958).

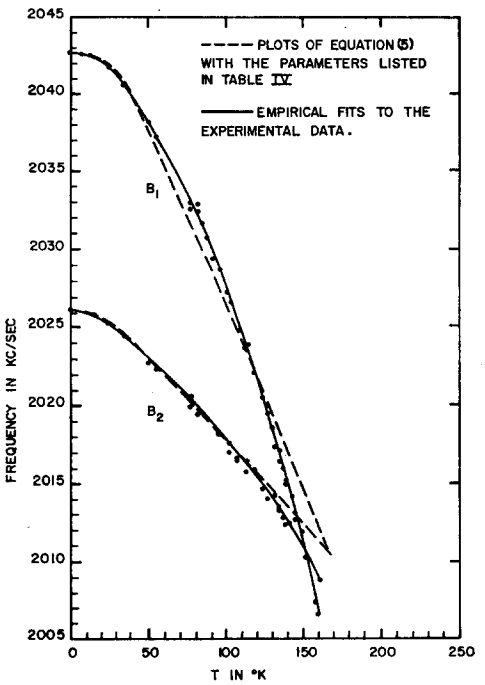

FIG. 5. Temperature dependence of the low-frequency quadrupole resonance of Molecules (1) and (2) in thiourea.

and 5, a single frequency will be used. This is reasonably well justified by the quality of the fit obtained. The temperature dependence of NQR line frequencies A_1, B_1 and A_2, B_2 have been fitted with a function of the form

$$\nu=\nu'\{1-b[\tfrac{1}{2}+1/(e^x-1)]\},$$

where

$$x=h\nu_t/kT. \tag{5}$$

The parameters found to make Eq. (5) fit the data are given in Table IV. There is a greater curvature in the empirical curve than in the single Einstein oscillator curve, indicating the presence of other oscillators less effective in averaging the field gradient at low temperatures. The errors in ν_t, ν', and b are estimated to be 20, 0.1, and 5%, respectively.

A plot of the asymmetry parameters η_1 and η_2 as a function of temperature for Molecules (1) and (2) are given in Fig. 6. The temperature coefficients b of the upper and lower transition frequencies associated with the nitrogen spectra of Molecule (1) are nearly equal while the temperature coefficients associated with Molecule (2) differ by a factor of 2.5. This difference in temperature coefficients is reflected in the temperature dependence of η for the respective molecular nitrogen sites.

The fact that the coefficients of $\langle\theta_x^2\rangle$, $\langle\theta_y^2\rangle$, and $\langle\theta_z^2\rangle$ are different in the expressions for ν_+ and ν_- suggests a geometrical interpretation.

Since there are only two pieces of information, b and ν_t, to be obtained from the data and six unknowns, it is impossible to make a definite statement on the x, y, or z rotational vibration dependence.

TABLE IV. NQR temperature-dependence parameters.

NQR Line	Molecule	ν_t (cps)	ν' (kc/sec)	b
A_1	(1)	2.1×10^{12}	2681.0	13.7×10^{-3}
B_1	(1)	1.9×10^{12}	2054.4	11.5×10^{-3}
A_2	(2)	1.7×10^{12}	2646.4	6.39×10^{-3}
B_2	(2)	1.0×10^{12}	2028.8	2.54×10^{-3}

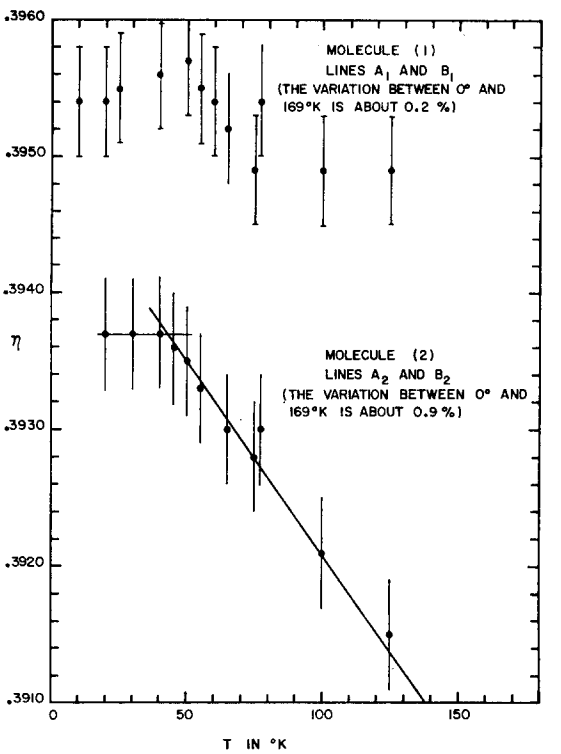

FIG. 6. The temperature dependence of the axial asymmetry parameters of Molecules (1) and (2) in thiourea.

C. Field-Dependent Effects of Nitrogen–Hydrogen Nuclear Dipole Coupling

1. Energy Levels

During the course of the experiments to determine the directions of the principal axes of the electric field gradient at the nitrogen nuclei, it became increasingly evident that normal magnetic field effects expected for the Zeeman shifts were not all that was being observed. A calculation of the Zeeman perturbation of the pure NQR spectra indicates that the frequency should shift as the square of the magnetic field H_0. The unexpected effects were deviations from the anticipated straight-line fit on the NQR frequency shift vs H_0^2. A plot illustrating this effect, which appears as a "wiggle," is given in Fig. 7. It is readily seen that the center of the wiggle comes at a magnetic field which

makes the splitting of the proton magnetic-dipole system equal to the difference in energy between the upper two nitrogen quadrupole levels. The deviations from the straight-line fits are such that the high-frequency lines for both spectra, the two pairs of upper curves, shift positively and then negatively as H_0 is increased while the low-frequency lines, the two lower curves, shift in the opposite sense.

It is expected that whenever the proton splitting is equal to the spacing between two energy levels of the nitrogen nucleus, one would observe some enhanced coupling. The theory of magnetic dipolar perturbation between the nitrogen and hydrogen nuclei demonstrates many of the observations and conjectures made.

The nitrogen and hydrogen nuclear spin energy levels are shown as a function of the magnetic field in Fig. 8, which shows that the nitrogen nuclear levels change very slowly in this field range compared to the strong field dependence of the proton spin system. Hence, for the purposes of discussion, the nitrogen nuclear levels are assumed to be essentially independent of magnetic field.

The dipole–dipole coupling between nitrogen and hydrogen nuclei is treated as a perturbation on the nitrogen quadrupole and hydrogen (proton) Zeeman systems. Accordingly, the wavefunctions used to describe the total unperturbed system are simple products of the wavefunctions associated with each system. This assumes that the applied magnetic field H_0 is large enough to make the proton Zeeman energy $H_0\gamma_p\hbar$ considerably larger than the dipolar coupling energy characterized by $\hbar^2\gamma_p\gamma_N/r^3$. The gyromagnetic ratios

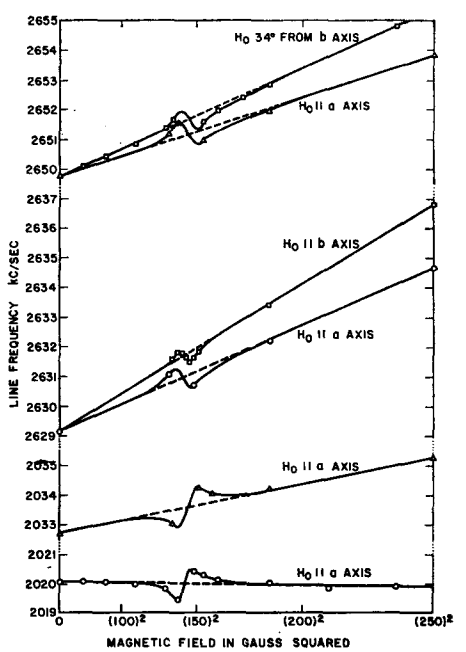

FIG. 7. The low-field dependence of the nuclear quadrupole resonance frequencies showing a wiggle which results from the nitrogen–hydrogen nuclear dipolar interaction.

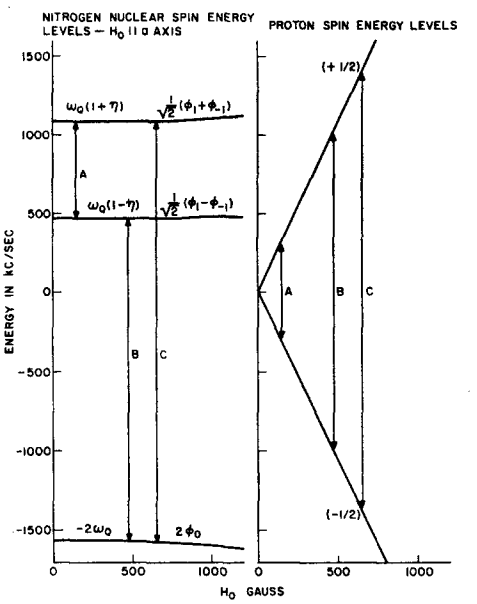

FIG. 8. Nitrogen and hydrogen nuclear spin energy level dependence on a low external magnetic field.

for protons and nitrogen nuclei are given by γ_p and γ_N, respectively. The magnetic fields for which the perturbation calculation will be used are large enough to satisfy the condition, and the quadrupole coupling constant $\hbar\omega_Q$ also satisfies the above condition. For the combined six-level system the following wavefunctions and energy levels are obtained:

Wavefunctions	Energy
$u_1=\psi_1 s$	$E_1\hbar^{-1}=\omega_Q(1+\eta)/4+\frac{1}{2}\omega_H$
$u_2=\psi_1 t$	$E_2\hbar^{-1}=\omega_Q(1+\eta)/4-\frac{1}{2}\omega_H$
$u_3=\psi_2 s$	$E_3\hbar^{-1}=\omega_Q(1-\eta)/4+\frac{1}{2}\omega_H$
$u_4=\psi_2 t$	$E_4\hbar^{-1}=\omega_Q(1-\eta)/4-\frac{1}{2}\omega_H$
$u_5=\psi_3 s$	$E_5\hbar^{-1}=\omega_Q(-2)/4+\frac{1}{2}\omega_H$
$u_6=\psi_3 t$	$E_6\hbar^{-1}=\omega_Q(-2)/4-\frac{1}{2}\omega_H.$

The nitrogen nuclear quadrupole wavefunctions ψ_1, ψ_2, and ψ_3 are defined in Sec. III. The usual spinup and spindown wavefunctions for the spin $-\frac{1}{2}$ proton system are represented by s and t.

The dipole–dipole Hamiltonian[8] $\mathcal{H}_{DD}$ is written

$$\mathcal{H}_{DD}=(\hbar^2\gamma_p\gamma_N/r_3)\{{}_H\mathbf{I}^N\cdot{}_N\mathbf{I}-[3(\mathbf{I}\cdot\mathbf{r})({}_H\mathbf{I}^N\cdot\mathbf{r})/r^2]\},$$

where ${}_NI$ and ${}_HI^N$ are the nitrogen and proton angular momentum operators written in terms of the nitrogen electric field gradient principal axes coordinates. The internuclear distance is given by r. The most distinguishing feature of this problem is that the axes of quantization for the nitrogen, z principal axis, and hydrogen (H_0) nuclei do not necessarily coincide. The linear rotational transformation A^{-1} is used to relate the components of proton angular momentum, parallel

TABLE V. The terms in ΔE_i that become large for certain values of ω_H with energy denominators written in angular frequency units.

$$\Delta E_1=(\hbar^2\gamma_p\gamma_N{}^2/r^3)\{\cdots\text{None}\cdots\}$$

$$\Delta E_2=(\hbar^2\gamma_p\gamma_N{}^2/r^3)\times\{[|H'_{32}|^2/(\omega_+-\omega_-)-\omega_H]+\cdots+[|H'_{52}|^2/(\omega_--\omega_H)]\}$$

$$\Delta E_3=(\hbar^2\gamma_p\gamma_N{}^2/r^3)\{-[|H'_{32}|^2/(\omega_+-\omega_-)-\omega_H]+\cdots\}$$

$$\Delta E_4=(\hbar^2\gamma_p\gamma_N{}^2/r^3)\{\cdots+[|H'_{54}|^2/(\omega_--\omega_H)]+\cdots\}$$

$$\Delta E_5=(\hbar^2\gamma_p\gamma_N{}^2/r^3)\times\{\cdots-[|H'_{54}|^2/(\omega_--\omega_H)]+\cdots-[|H'_{52}|^2/(\omega_+-\omega_H)]\}$$

$$\Delta E_6=(\hbar^2\gamma_p\gamma_N{}^2/r^3)\{\cdots\text{None}\cdots\}$$

and perpendicular to the externally applied magnetic field, to the components of angular momentum along the electric field gradient principal axes. The transformation A^{-1} can be expressed in terms of Euler angles[9] θ, ϕ', and ψ'. The first two angles specify the position of the applied magnetic field H_0, while ψ' describes the precession of the proton angular momentum about H_0. Since ψ' is arbitrary and must drop out of the calculation, it is set equal to zero for the sake of convenience. The components of the proton angular-momentum operators ${}_HI_{x_i}{}^N$ in the nitrogen coordinates can be written in terms of the operators in the proton system ${}_HI_{x_j}{}^H$ as follows:

$$\begin{aligned}
{}_HI_x{}^N&=(\cos\psi'\cos\phi'-\cos\theta'\sin\phi'\sin\psi'){}_HI_x{}^H\\
&\quad+(-\sin\psi'\cos\phi'-\cos\theta'\sin\phi'\cos\psi'){}_HI_y{}^H\\
&\quad+\sin\theta'\sin\phi'{}_HI_z{}^H,\\
{}_HI_y{}^N&=(\cos\psi'\sin\phi'+\cos\theta'\cos\phi'\sin\psi'){}_HI_x{}^H\\
&\quad+(-\sin\psi'\sin\phi'+\cos\theta'\cos\phi'\cos\psi'){}_HI_y{}^H\\
&\quad-\sin\theta'\cos\phi'{}_HI_z{}^H,\\
{}_HI_z{}^N&=\sin\theta'\sin\psi'{}_HI_x{}^H+\sin\theta'\cos\psi'{}_HI_y{}^H+\cos\theta'{}_HI_z{}^H.
\end{aligned}$$

The internuclear vector $\mathbf{r}$ can be specified by its magnitude r and three direction cosines α, β, and δ written relative to the x, y, and x principal axis system $\mathbf{r}=r(\alpha_i+\beta_j+\delta_k)$. In the present case, $\mathbf{r}$ is approximately in the x, y plane; therefore, δ is small and taken to be zero for this problem.

All of the diagonal matrix elements of $\mathcal{H}_{DD}$ are zero in the u_1, u_2, $\cdots$, u_6 representation. Therefore there is no first-order N–H dipolar broadening, just as there is no first-order Zeeman shift of the nitrogen nuclear energy levels. The calculation of the second-order dipolar coupling is very involved, and only those terms pertinent to the discussion are considered. An estimate of the second-order dipolar broadening can be obtained from the relation, $\Delta\nu=(\pi)^{-1}(\mathcal{H}_{DD})^2(\eta\hbar\omega_Q)^{-1}\approx 300\ \text{sec}^{-1}$, which agrees well with observed widths. The nonzero matrix elements of $\mathcal{H}_{DD}$ are as follows, where $H_{ij}'=(\mathcal{H}_{DD})_{ij}(r_3/\hbar^2\gamma_p\gamma_N)$ and $H_{ij}'=H_{ji}'^*$:

$$\begin{aligned}
H_{31}'&=\tfrac{1}{2}(\cos\theta'),\\
H_{41}'&=\tfrac{1}{2}(i\sin\theta'),\\
H_{51}'&=\tfrac{1}{2}[\sin\theta'\sin\phi'-3\alpha(\alpha\sin\theta'\sin\phi'-\beta\sin\theta'\cos\phi')],\\
H_{61}'&=\tfrac{1}{2}\{\cos\phi'-i\cos\theta'\sin\phi'-3\alpha[\alpha(\cos\phi'-i\cos\theta'\sin\phi')\\
&\qquad+\beta(\sin\phi'+i\cos\theta'\cos\phi')]\},\\
H_{32}'&=\tfrac{1}{2}(-i\sin\theta'),\\
H_{42}'&=\tfrac{1}{2}(-\cos\theta'),\\
H_{52}'&=\tfrac{1}{2}\{(\cos\phi'+i\cos\theta'\sin\phi')\\
&\qquad-3\alpha[\alpha(\cos\phi'+i\cos\theta'\sin\phi')\\
&\qquad+\beta(\sin\phi'-i\cos\theta'\cos\phi')]\},\\
H_{62}'&=\tfrac{1}{2}[-\sin\theta'\sin\phi'\\
&\qquad-3\alpha(-\alpha\sin\theta'\sin\phi'+\beta\sin\theta'\cos\phi')],\\
H_{53}'&=\tfrac{1}{2}[-i\sin\theta'\cos\phi'\\
&\qquad-3i\beta(\alpha\sin\theta'\sin\phi'-\beta\sin\theta'\cos\phi')],\\
H_{63}'&=\tfrac{1}{2}\{(-\cos\theta'\cos\phi'+i\sin\phi')\\
&\qquad-3\beta[\alpha(-\cos\theta'\sin\phi'+i\cos\phi')\\
&\qquad+\beta(-\cos\theta'\cos\phi'+i\sin\phi')]\},\\
H_{54}'&=\tfrac{1}{2}\{\cos\theta'\cos\phi'+i\sin\phi'\\
&\qquad-3\beta[\alpha(-\cos\theta'\sin\phi'+i\cos\phi')\\
&\qquad+\beta(\cos\theta'\cos\phi'+i\sin\phi')]\},\\
H_{64}'&=\tfrac{1}{2}[i\sin\theta'\cos\phi'\\
&\qquad-3i\beta(-\alpha\sin\theta'\sin\phi'+\beta\sin\theta'\cos\phi')]. \qquad (6)
\end{aligned}$$

The second-order perturbation which results is of the usual form

$$\Delta E_j=\sum_{i\neq j}[|H_{ji}'|^2/(E_j-E_i)],$$

and only those terms with energy denominators E_j-E_i which can become small for certain values of ω_H are of interest here. These terms will dominate the broadening and shifting of the nitrogen resonance line. It should be noted that the values of ω_H that make the energy denominators small are those at which the proton Larmor frequency equals one of the nitrogen quadrupolar transition frequencies, and at these values of ω_H, hydrogen and nitrogen nuclei can engage in mutual spin flips that conserve energy. The terms in ΔE_j of importance of this discussion are given in Table V with energy denominators written in angular frequency units.

The only observed wiggle in the Zeeman effect occurs when the applied field makes $|E_2-E_3|\approx 0$. The high-frequency transition ν_+ consists of transitions from levels E_1 to E_5 and E_2 to E_6. Only terms involving

$|H_{32}'|^2$ are large as ω_H approaches $(2\omega_Q\eta)/4$ [and (E_2-E_3) approaches zero]. It can be seen from Table V that the transition involving E_1 to E_5 is unchanged and the transition E_2 to E_6 is shifted *up* in frequency when $\omega_H<(2\omega_Q\eta)/4$. The low-frequency transition ν_- consists of E_3 to E_5, which is shifted down in frequency when $\omega_H<(2\omega_Q\eta)/4$, and E_4 to E_6 which is unchanged. The different sign of the wiggle for the high- and low-frequency transitions is due to the differing signs of the perturbation terms E_2 and E_3. Similar effects should occur at $\omega_H\approx\omega_+$ and $\omega_H\approx\omega_-$, but we did not search for them.

As the critical value of ω_H is approached, the dipolar coupling not only splits the resonance but also shifts the center of gravity of the line. A shift of a resonance due to dipole–dipole coupling is unusual and is a consequence of the fact that in this system the first-order dipolar coupling is zero and the shift is a second-order perturbation effect. The shift is observable here because of the narrow nitrogen resonance linewidth. At the values of ω_H which make the energy denominator very small, the second-order theory breaks down, and the line is broadened to a width of approximately $\Delta\omega=(\hbar\gamma_p\gamma_N)r^{-3}$, or about 10 times the zero-field linewidth. The resonance is unobservable in this region of applied field.

2. *Dynamic Effects*

The enhanced dipolar coupling expressed in the $|H_{52}'|$ terms of the equations in Table V has been observed through cross-relaxation effects on the proton NMR system. At the temperatures used in this experiment, the proton thermal relaxation time, ${}_HT_1$ ranges from 5 min to more than an hour. It is possible to saturate the proton spin system at a high magnetic field (arbitrarily chosen to be 1.6 kG), lower the external magnetic field until level crossings corresponding to zero energy denominators in Column 3 are reached, and then return again to the high field to observe a recovery of the proton spin system due to fast cross relaxation with the nitrogen systems at the lower field. The lower field used is called the "soak field" and is about 610 G in thiourea. The signal proportional to the magnetization of the proton spin system is observed at 1.6 kG as the height of the free-induction decay following a 90° pulse in the fixed-frequency pulsed NMR apparatus (pulse rig).

In the temperature range 77° to 165°K the nitrogen spin-lattice relaxation time ${}_NT_1$ ranges from about 20 to 6 sec, respectively, the cross-relaxation rate due to N–H dipolar coupling is the order of $W_0\approx\hbar\gamma_p\gamma_N(r^{-3})\approx 2\times10^{+4}$ sec^{-1}. Therefore, $W_0\gg1/{}_NT_1\gg1/{}_HT_1$.

Since there is strong dipolar coupling within the proton spin system, the recovery process can be described in terms of spin temperatures. At the high field the proton system has a high spin temperature T_{HS} after saturation. In a very short time ($\sim W_0^{-1}$) after level crossings are reached at 610 G, T_{HS} is lowered by exchange with the nitrogen system and the spin temperature of the nitrogen system, and T_{NS} is correspondingly raised.

If the external field is then kept fixed at 610 G, both the proton and nitrogen spin systems relax through the nitrogen spin–lattice relaxation mechanism and T_{NS} and T_{HS} approach the lattice temperature T. Since ${}_HT_1$ is much greater than ${}_NT_1$, the recovery of the proton system by its own relaxation mechanisms can usually be neglected. Finally, when the field is again raised to 1.6 kG for measurement of the proton magnetization, the proton spin system is adiabatically magnetized and its temperature is increased by a factor equal to the ratio of external fields $1.6\times10^3/610$, or a factor of about 2.62 over the last value of T_{HS} at 610 G.

That the effect exists can be observed by using a very short "soak time" at various soak fields below 1.6 kG and by observing the partially cooled proton spin system at 1.6 kG. Second, by varying the soak time at 610 G, the rate with which T_{HS} approaches the lattice temperature T can be determined, and the nitrogen spin-lattice relaxation time can be obtained. A third useful observation is that the proton magnetization, after a long soak time ($\gg{}_NT_1$) will be recorded as a signal at 1.6 kG, which is a factor of $(2.62)^{-1}$ times the equilibrium proton magnetization at that field. This measurement is of practical importance in the experimental determination of ${}_HT_1$, for it means that the equilibrium proton magnetization can be measured in a few minutes instead of an otherwise long wait of several hours when ${}_HT_1$ is itself about one hour.

Figure 9 shows a plot of recovered proton polarization as a function of "soak field." No recovery effects are observed above 660 G, and the effect is complete at about 610 G where the proton Larmor frequency approximately equals the quadrupole transition frequencies ν_+ of Molecules (1) and (2). It is not possible, with the apparatus used, to pass through the ν_+ level crossings rapidly enough to avoid energy exchange with the nitrogen system. If this were possible, another peak in recovery would show at a field of about 480 G where the proton Larmor frequency would equal ν_-. With a soak time of 30 sec at 83°K, the soak time was long compared to passage times through level crossings, but also long enough to allow weaker, higher-order cross-relaxation effects to show, so that there is no resolution of ν_+ and ν_- peaks in Fig. 9. At 198°K, ${}_HT_1$ is about 5 min, and correction for proton direct spin-lattice relaxation has been made. The evidence in Fig. 9 of proton recovery at a high-field value of 800 G indicates that at 198°K the nitrogen quadrupole transitions are very broad, which is consistent with the fact that no pure NQR has been observed above 169°K. The broadening must be associated with the onset of molecular motion at 169°K. Other known phase transitions at 176°, 180°, and 202°K complicate interpretation here.

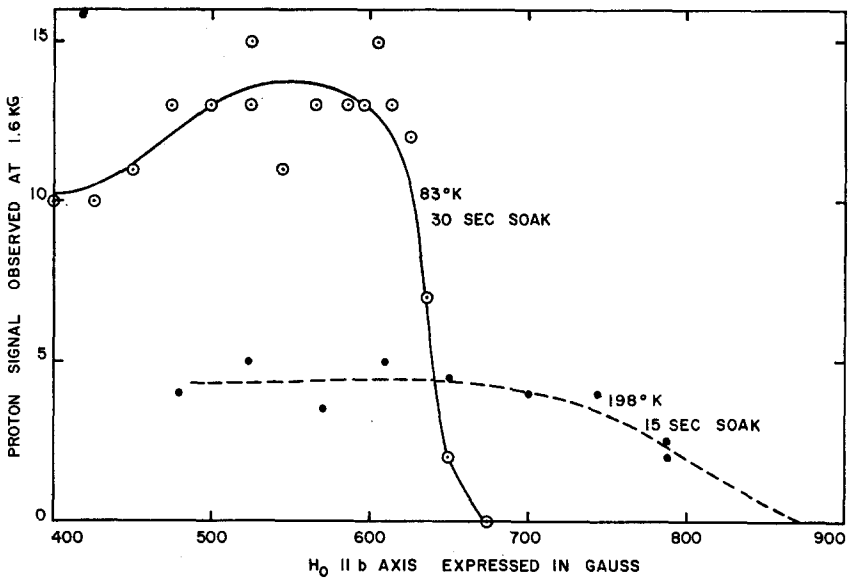

FIG. 9. Recovery of an initially saturated proton spin system after a fixed period of time is spent at various external magnetic fields.

The technique employed in obtaining data for Fig. 10 could prove useful in finding nuclear quadrupole transition frequencies in other nitrogen compounds that contain hydrogen. In temperature regions where the proton spin-lattice relaxation time is very long, the proton system acts as a variable frequency probe which carried energy through the frequency spectrum when the magnetic field is changed. This technique would be most useful in systems where the nitrogen interaction lacks axial symmetry and would have a small Zeeman perturbation.

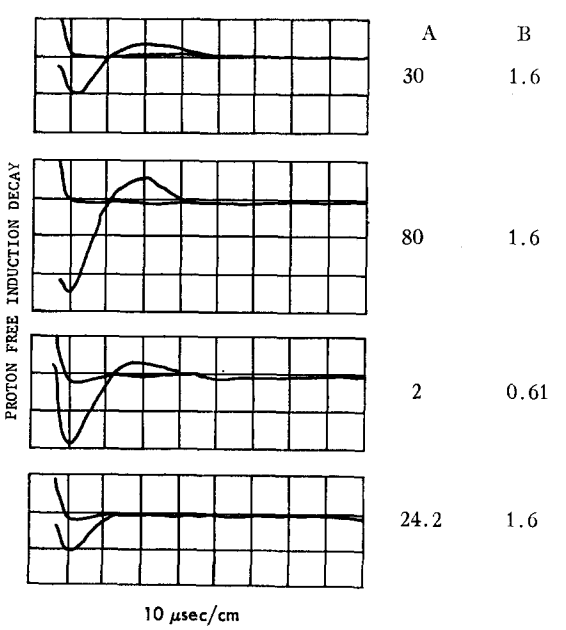

A—Time after 90° pulse at 1.6 kG (min.)
B—Soak Field (kG)
Proton $_HT_1 \approx 2$ h at 1.6 kG
$T = 163°K$
NQR Relaxation Time~6 sec.

FIG. 10. Oscilloscope traces of proton spin resonance free induction decay. The difference between the two traces on each grid is a measure of the amount of proton spin polarization.

Similar techniques have been employed to determine the chlorine electric quadrupole interactions in $Ba(ClO_3)_2 \cdot H_2O$.[13]

With the soak field set for maximum enhancement of the dipolar interaction, the nitrogen thermal relaxation rates $(_NT_1)^{-1}$ control the rate of recovery of the proton polarization during the "soak time." An example is given in Fig. 10 of the free induction decay observed after a 90° pulse, where the proton system has been previously saturated by a 90° pulse. (The amplitude of the downward portion of the curve is proportional to the polarization recovered.) Note the rapid relaxation at 610 G. The relaxation time of the nitrogen quadrupole system is about 6 sec (measured via proton polarization and spin mixing) at a temperature of 163°K.

At certain values of the external field, such as 610 G, there is good thermal contact between spin systems; and the rate of change of spin temperature or of proton magnetization can be developed as follows. Let δ_i represent the deviation from equilibrium differences in population between two energy levels, and let W_i be the corresponding spin–lattice relaxation transition rate coupling levels, labeled a, b, c, d, e, as shown in the diagram of Fig. 11 ($i=1, 2, 3, 4$). Finally, let the mutual spin flip rate due to the dipole–dipole interaction be given by W_0. For external applied fields that

[13] S. Nakamura and H. Enokiya, J. Phys. Soc. Japan **18**, 193 (1963).

make $\omega_H \approx \omega_+$, the rate equations can be written as

$$d\delta_1/dt = -2W_1\delta_1 + W_2\delta_2 - W_3\delta_3 - W_0[\delta_3 - \delta_4/3],$$
$$d\delta_2/dt = W_1\delta_1 - 2W_2\delta_2 - W_3\delta_3 - W_0[\delta_3 - \delta_4/3],$$
$$d\delta_3/dt = -W_1\delta_1 - W_2\delta_2 - 2W_3\delta_3 - 2W_0[\delta_3 - \delta_4/3],$$
$$d\delta_4 = +2W_0[-\delta_4/3 + \delta_3]. \quad (7)$$

The normal relaxation rate W_4 has been left out since in thiourea at $T<165°$K, $W_4 \ll W_1$, W_2, W_3. The Eqs. (7) have been written for thiourea in which the ratio R of number of protons to nitrogen nuclei is $R=2$. For any other system, the coefficient of δ_4 would be $(2/3R)$ instead of $(\frac{1}{3})$ as it appears above. In thiourea the proton linewidth is so large that it "covers" the values of ω_+ for Molecules (1) and (2), and for the purposes of this discussion it can be assumed that both molecules have equal quadrupole interactions. It should also be noted that there are actually only three independent equations for the δ_i since the values of δ_i for nitrogen are related by $\delta_3 = \delta_2 + \delta_1$.

Now, since $W_0 \gg W_i$, rapid changes in δ_3 and δ_4 occur until $\delta_4 = 3\delta_3$. It will be further assumed that δ_3 and δ_4 maintain this relationship due to the strong influence of W_0 as they approach zero.

The solution to the set of simultaneous Eqs. (7), under the above assumptions, is $\delta_3(t) = A\exp(\rho_\alpha t) + B\exp(\rho_\beta t)$, where

$$\rho_\alpha = -(W_1+W_2+W_3) - [W_1^2+W_2^2+W_3^2-(W_1W_2+W_1W_3+W_2W_3)]^{\frac{1}{2}},$$
$$\rho_\beta = -(W_1+W_2+W_3) + [W_1^2+W_2^2+W_3^2-(W_1W_2+W_1W_3+W_2W_3)]^{\frac{1}{2}},$$

and the constants A and B are determined by the initial conditions. The time $t=0$ is chosen as the time just after mutual spin flips at rate W_0 make $\delta_4 = 3\delta_3$ and before relaxation due to the other W_i become effective.

The proton system is, in this experiment, completely unpolarized when it is brought into "contact" with the level spacing, ω_+. Then after the spin flips due to W_0 occur, the initial conditions can be readily seen to be

$$\delta_4(0) = -\tfrac{1}{4}\Delta_3°,$$
$$\delta_3(0) = -\tfrac{3}{4}\Delta_3°,$$
$$\delta_2(0) = -\tfrac{3}{8}\Delta_3°,$$
$$\delta_1(0) = -\tfrac{3}{8}\Delta_3°,$$

where $\Delta_3°$ is the thermal eqiulibrium population difference between the nitrogen levels c and e. Only the solution for δ_3 has been given for the general case where $W_1 \neq W_2 \neq W_3$. In general the recovery will be characterized by two relaxation rates ρ_α and ρ_β.

If the assumption is made that all $\Delta m = \pm 1$ transition rates due to relaxation processes are equal, then, $W_2 = W_3$, and for the above initial conditions, $\delta_3(t) = \delta_4(t)/3 = -\frac{3}{16}\Delta_3°[\exp-(W_2+2W_1)t + 3\exp(-3W_2t)]$.

Unfortunately, the experimental data is not good enough to distinguish two exponentials in the decay of δ_4 to within a factor of 2 $W_1 \approx W_2$, and $({}_NT_1)^{-1} \approx 3W_1$.

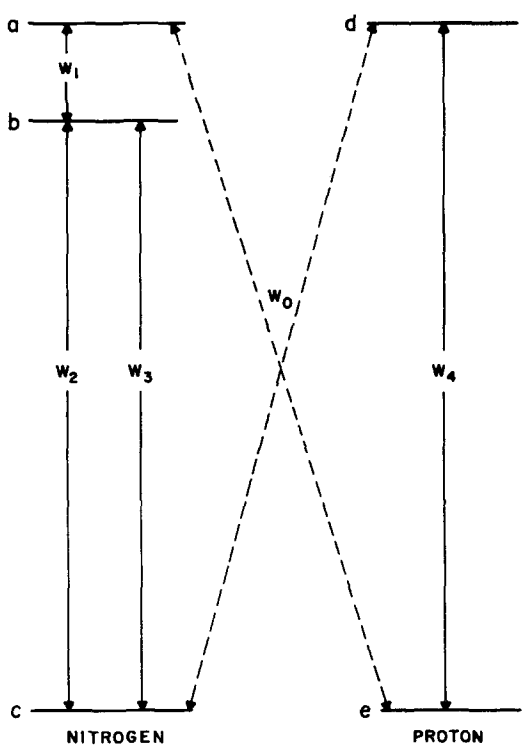

FIG. 11. Energy level diagram of nitrogen and single proton spin systems in an external magnetic field of 610 G which makes $\omega_H = \omega_+$. The solid arrows represent spin lattice relaxation rates and the dashed arrows represent dipole–dipole coupling rates.

D. Proton Spin–Lattice Relaxation

Measurements of the proton spin–lattice relaxation times $({}_HT_1)$ were carried out for thiourea between 77° and 400°K. The measurements were made with the pulsed nuclear magnetic resonance spectrometer using a sequential pair of 90° pulses and observing the amplitude of the free induction decay following the second pulse. The Larmor frequency was 6.95 Mc/sec. The relaxation times obtained at this Larmor frequency are given as a function of $1/T$ in Fig. 12.

The ${}_HT_1$ measurements below 169°K were somewhat uncertain because of the difficulty in establishing the equilibrium signal amplitude due to the long term equipment instabilities. Much of the difficulty was overcome, however, by using the effect of cross relaxation with the nitrogen quadrupole system as described in the previous section. If $S(t)$ is the signal amplitude at a time t after the first 90° pulse, a plot of $\ln[S(\infty) - S(t)]$ vs t determines ${}_HT_1$ as the reciprocal of the slope of the line.

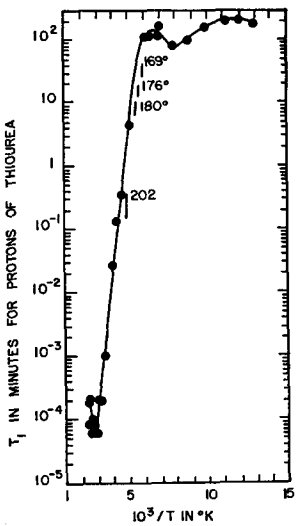

FIG. 12. Temperature dependtnce of proton spin-lattice relaxation time.

Powdered and single-crystal samples of thiourea gave the same values of ${}_HT_1$ indicating that the relaxation mechanism is essentially isotropic. Most of the samples used were single crystals because they provided better filling factors, longer free-induction decay times, and thus better signal to noise ratios. It is necessary to strive for the best signal-to-noise in these experiments because the broad proton line has a free-induction decay time of 20 μsec. Examples of the free induction decay are given in Fig. 10. Since the signal decays so rapidly after a pulse, a good deal of the signal is lost during the time it takes the spectrometer receiver to recover from overload.

The temperature dependence of ${}_HT_1$ between 169° and 400°K follows the form of the Bloembergen, Purcell, and Pound theory of relaxation.[14] Accordingly, an activation energy H and a pre-exponential frequency factor ν_0 have been determined from the slope and minimum in the ${}_HT_1$ curve. Another minimum appears near 125°K, but there is some question of its validity due to rather large errors (estimated to be around 30%) in the data. However, it has repeated itself on all of the runs.

The correlation time τ_c of the motion to which ${}_HT_1$ is sensitive is given by $\tau_c=(1/\nu_0)\exp(H/kT)$. A plot of τ_c is given in Fig. 11 for the two activation energies and frequency factors given in Table VI.

TABLE VI. Activation energies and frequency factors for protons in thiourea.

${}_HT_{1\min}$ Temperature (°K)	Activation energy (H)	Frequency factor (ν_0)
123	3.8×10^{-2} eV (0.88 kcal/mole)	2.3×10^{9} (sec^{-1})
346	0.43 eV, (10 kcal/mole)	7.5×10^{13} (sec^{-1})

[14] N. Bloembergen, E. M. Purcell, and R. V. Pound, Phys. Rev. **73**, 649 (1948).

This knowledge of τ_c versus temperature makes it possible to estimate the temperature at which the quadrupole resonance will be broadened by molecular motion. If the motion modulates the electric field gradient at the nitrogen nuclei by an amount which is much greater than the quadrupole resonance linewidth, then the onset of motion can broaden the line. When the correlation time becomes comparable to and less than the reciprocal of the original NQR linewidth, about 10^{-3} sec, the broadening due to molecular motion will be significant. This occurs at temperatures above 169°K and accounts for the lack of an observed resonance at $T>169$°K. The known crystal structure changes at 176°, 180°, and 202°K may introduce discontinuities in the quadrupole coupling constants and further complicate the quadrupole interaction. Since no nitrogen NQR resonance has been observed at 300°K where τ_c is about 10^{-7} sec, one can conclude that the depth of the modulation of ω_Q due to the motion must have an angular frequency of about 10^7 sec^{-1} or more.

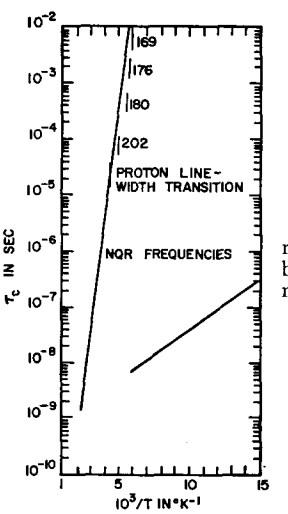

FIG. 13. Correlation times for molecular reorientation in thiourea based upon measured proton thermal relaxation times.

In their studies of the proton magnetic resonance in thiourea Emsley and Smith[4] find that the linewidth in a powdered sample changes from 9 to 14 G as the temperature is lowered past 230°K. The transition extends over a temperature range of about 20°. The line is assumed to be narrowed above the transition by an averaging of the dipolar coupling between protons as a result of thermal motion. The temperature corresponding to $\tau_c\approx(\omega_{\frac{1}{2}})^{-1}$, where $\omega_{\frac{1}{2}}$ is the linewidth of the proton absorption expressed in angular frequency units, should mark the approximate temperature of the linewidth transition. The correlation time for a linewidth reduction of 2.5 G is about 1.5×10^{-5} sec. This value for the correlation time occurs at about 230°K in agreement with the narrowing temperature observed by Emsley and Smith.

The correlation time curve, see Fig. 13, based on the high-temperature ${}_HT_1$ data is not extended to tem-

peratures below 169°K since the plot of $\log {}_H T_1$ vs $1/T$, see Fig. 11, does not continue as a straight line below $T=169$°K.

The temperature dependence of the ${}_H T_1$ data and the intensity of the NQR data indicate that the ferroelectric transition temperature, 169°K, marks the onset of thermal motion in this crystal.

The leveling off of ${}_H T_1$ around 90°K is not unexpected. At that temperature ${}_H T_1$ is so long that a slight amount of paramagnetic impurity might serve to relax the system more efficiently than the proton–proton dipolar motion. Furthermore, the quadrupole relaxation time is still increasing rapidly in this temperature region. (Discussion of the quadrupole relaxation times is deferred to the next section.) On the basis of an order of magnitude spin-diffusion calculation, a concentration of only 10^{13} relaxation centers per cubic centimeter is necessary for a ${}_H T_1$ ceiling of 200 min. Such a small concentration of relaxation centers would be pressing the sensitivity of an electron spin resonance spectrometer even if they were all centers with the same g value. An electron spin resonance search in the region of $g=2$ did not reveal anything.

E. Nitrogen Quadrupolar Relaxation

The nitrogen quadrupole level system is observed to have a spin-lattice relaxation time that depends on temperature approximately as $T_1 \propto (T)^{-2}$. A plot of T_1 vs T appears in Fig. 14. At temperatures above 77°K, spin mixing experiments described above were used to measure the relaxation time via the proton recovery. In this temperature range, the low-level oscillator used did not have enough power to saturate the resonance and it was not used to measure T_1. Below 77°K, the oscillator operating at a high level could saturate the resonance. The recovery of the signal after saturation was observed at a low rf level. This data was used to determine ${}_N T_1$ of the upper and lower transitions directly, and it was found that their relaxation rates were about equal, within a factor of two.

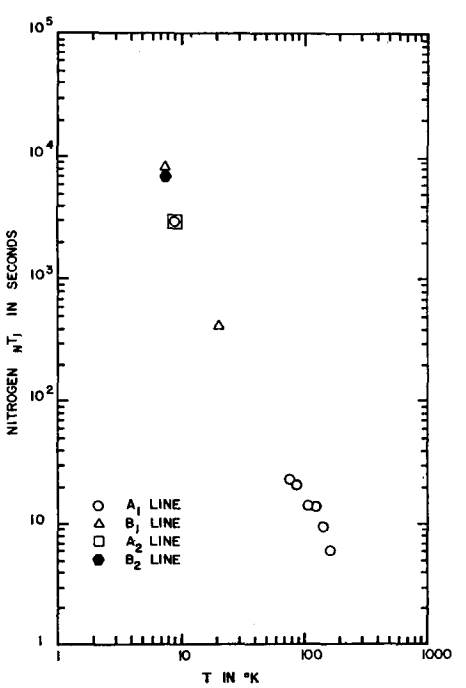

FIG. 14. Temperature dependence of nitrogen spin–lattice relaxation time.

V. CONCLUSION

The coupling constants of the nitrogen quadrupole systems provide qualitative information on the charge distribution responsible for the electric field gradient. However, the changes in the coupling constant with temperature and the directions of the principal axes of the electric field gradient can provide rather definite information on the crystal structure.

Zeeman perturbation experiments identify two sets of molecules, one associated with each set of nitrogen quadrupole spectra; they are referred to as 19.4° and 29.5° molecules which may be a misnomer because the x-ray data on which these labels are based was taken at 120°K,[1] whereas the NQR data is at 77°K. The z principal axes are approximately 17° and 33° relative to the b axis and perpendicular to the c axis at 77°K. If one assumes that the xy principal axis plane is coplanar with the molecule, then the above data leads one to conclude that the average positions of the two molecules are different at 77° and 120°K. However, from some approximate experimental checks of the principal axis directions at 157°K appear to be the same as those found at 77°K.

The x principal axis is found to be out of alignment with the C,N bond direction, the axis of symmetry in the NH_2 group. This rotation (12° or 18° depending on the molecule in question) is not adequately explained by elementary hybrid atomic bond orbital models and the dipole moment of the molecule.

The two highest-frequency transitions in each quadrupole spectrum exhibit temperature dependences that follow Bayer's theory of electric-field gradient averaging by Einstein local harmonic oscillators. The electric-field gradient asymmetry parameter is approximately 40% showing only a small temperature variation for Molecule (1) and a definite 1% decrease for Molecule (2) between 10° and 130°K. The molecule urea is similar to thiourea but in the solid, the nitrogen nuclear quadrupole interaction has an axial asymmetry parameter of only 32%.[10] An attempt has been made here to associate the large asymmetry parameter in thiourea with the angular displacement of the x principal axis from the C,N bond direction.

The magnetic dipolar coupling between the nitrogen and neighboring hydrogen nuclei can cause mutual spin flips to occur between the nitrogen and proton systems if the applied magnetic field is adjusted to a value

which equates the proton frequency and one of the quadrupole transition frequencies in a given energy level scheme. Thus, the dipolar coupling provides a useful tool with which to study the relaxation mechanisms of the nitrogen quadrupole and proton systems via the proton polarization recovery (direct proton-lattice relaxation times are ~ 2 h) with a pulsed nuclear magnetic resonance spectrometer.

The proton spin–lattice relaxation times exhibit a temperature dependence due to molecular motion consistent with previous work on thiourea,[4] where it was concluded that there is hindered rotation about the S,C bond, between approximately 175°K and the decomposition temperature of 433°K. The values of proton T_1 found for thiourea were considerably longer than those previously reported.[4] The extremely long proton relaxation times at temperatures below 170°K indicate that there is only a small amount of thermal motion affecting the protons. In addition the correlation time data provide an explanation for the lack of an observed nitrogen quadrupole resonance above 169°K.

ACKNOWLEDGMENTS

The authors appreciate helpful comments from G. J. Goldsmith, R. H. Silsbee, D. Zamir, and D. F. Holcomb. D. H. McMahon kindly examined some thiourea samples by electron spin resonance. Mrs. P. Griffith assisted with the computer program.

THE JOURNAL OF CHEMICAL PHYSICS VOLUME 41, NUMBER 8 15 OCTOBER 1964

Boundary Conditions and the Anharmonic Contributions to the Free Energy of a Lattice

P. LLOYD AND J. J. O'DWYER
School of Physics, University of New South Wales, Kensington, New South Wales, Australia

(Received 25 May 1964)

In the evaluation of the free energy of a lattice in the harmonic approximation it is well known that the results are, to thermodynamic accuracy, independent of the boundary conditions used. It is shown here, by way of a simple example, that this is not so in the evaluation of the anharmonic contributions to the free energy. Physically the difference corresponds to whether or not the lattice is free to expand, or is constrained to a fixed volume, for the differing temperatures at which the partition function is evaluated.

IN the evaluation of the free energy of a lattice in the harmonic approximation it is well known[1] that the use of differing boundary conditions on the lattice does not alter the result to within thermodynamic accuracy. A consequence of this is that cyclic boundary conditions are invariably used, for although they are quite artificial, they possess the most convenient mathematical properties. Recently there have been several calculations[2–7] of the anharmonic contributions to the free energy of a lattice. In these cases, cyclic boundary conditions have also been used although it is not so certain in this case that the results will be independent of the boundary conditions. In fact Stern[2] asserts that he has calculated the anharmonic contribution to the Gibbs free energy at zero pressure while the other authors state that they have calculated the anharmonic contribution to the Helmholtz free energy at a constant volume. By considering a simple example of a linear chain, we wish to show that the anharmonic contribution to the free energy does depend on the boundary conditions. If the boundary conditions are appropriate to a constant volume, then the anharmonic contribution calculated is the contribution to the Helmholtz free energy at that volume, while if the boundary atoms are constrained then the anharmonic contribution to the Gibbs free energy at zero pressure is calculated. The use of artificial cyclic boundary conditions appears to yield the anharmonic contribution to the Helmholtz free energy as stated by the majority of authors quoted.

The constant pressure partition function,[8] which gives rise to the Gibbs free energy, and the constant volume partition function which gives rise to the Helmholtz free energy, are apparently identical if the external pressure is zero. In the classical limit the configuration partition function is given by

$$e^{-\beta X}=\int\cdots\int e^{-\beta U}d^{3N}x, \tag{1}$$

where $\beta=1/kT$ is the inverse temperature, and X is the configurational part of the Helmholtz free energy, F in the constant volume case, while X is the configura-

[1] M. Born and K. Huang, *Dynamical Theory of Crystal Lattices* (Clarendon Press, Oxford, England, 1956), Appendix 4.
[2] E. A. Stern, Phys. Rev. **111**, 786 (1958).
[3] G. Leibfried and W. Ludwig, Solid State Phys. **7**, 275 (1961).
[4] A. A. Maradudin, P. A. Flinn, and R. A. Coldwell-Hersfall, Ann. Phys. (N.Y.) **15**, 337, 360 (1961).
[5] J. M. Keller and D. C. Wallace, Phys. Rev. **126**, 1275 (1962).
[6] P. A. Flinn and A. A. Maradudin, Ann. Phys. (N.Y.) **22**, 223 (1963).
[7] D. C. Wallace, Phys. Rev. **131**, 2046 (1963).
[8] P. Lloyd and J. J. O'Dwyer, Mol. Phys. **6**, 573 (1963).